Chapter

Fluorescent Markers: Proteins and Nanocrystals

Anielle Christine Almeida Silva, Jerusa Maria de Oliveira, Kelen Talita Romão da Silva, Francisco Rubens Alves dos Santos, João Paulo Santos de Carvalho, Rose Kethelyn Souza Avelino, Eurípedes Alves da Silva Filho, Marcelo Duzzioni, Edigar Henrique Vaz Dias, Fábio de Oliveira, Juliana Rodrigues Machado, Malu Mateus Santos, Marcos Vinícius da Silva, Carlo José Freire de Oliveira, Virmondes Rodrigues Junior, Lucas Anhezini and Noelio Oliveira Dantas

Abstract

This book chapter will comment on fluorescent reporter proteins and nanocrystals' applicability as fluorescent markers. Fluorescent reporter proteins in the Drosophila model system offer a degree of specificity that allows monitoring cellular and biochemical phenomena *in vivo*, such as autophagy, mitophagy, and changes in the redox state of cells. Titanium dioxide (TiO_2) nanocrystals (NCs) have several biological applications and emit in the ultraviolet, with doping of europium ions can be visualized in the red luminescence. Therefore, it is possible to monitor nanocrystals in biological systems using different emission channels. CdSe/CdS magic-sized quantum dots (MSQDs) show high luminescence stability in biological systems and can be bioconjugated with biological molecules. Therefore, this chapter will show exciting results of the group using fluorescent proteins and nanocrystals in biological systems.

Keywords: nanocrystals, fluorescent proteins, fluorescent markers, magic-sized quantum dots, titanium dioxide

1. Introduction

Several types of tools have been developed in order to monitor biological processes through fluorescence images. Some of these tools are the use of fluorescent proteins and nanomaterials. This book chapter will comment in particular on green fluorescent protein and luminescent nanocrystals.

The green fluorescent protein (GFP) of Jellyfish *Aequoria victoria* and fluorescent homologous proteins of different colors isolated from other sea creatures have led to the development of fluorophores that have been widely used in recent

decades. In the biological area, fluorescent antibodies are a powerful tool for analyzing the subcellular location of proteins of interest. In addition, a gene encoding a fluorescent protein can be introduced into a model organism, resulting in the expression of functional fluorescent proteins, which can then be detected by fluorescence microscopy, flow cytometry, and other fluorescence-based methods. Fluorescent proteins have revolutionized biological and biomedical research, for example, it is possible to monitor the activity of a gene promoter by placing a fluorescent protein under its control. By using this tool, the spatial and temporal patterns of gene activation were revealed, as well as it was possible to trace the specific fates of cell populations or even to visualize the different shapes that cells can assume during development. Perhaps the most sophisticated area is the construction of genetically modified fluorescent sensors for the detection of ions, small molecules, and various types of enzyme activity [1–3].

One of the best and most used *in vivo* models to investigate biological phenomena is the fruit fly. The fruit fly *Drosophila melanogaster* is a well-established model organism in nanotoxicology studies [4]. *Drosophila* has a short life cycle, low maintenance cost, and a considerable amount of conserved genes and physiological mechanisms with humans [5, 6]. The complete sequencing of the *Drosophila* genome combined with genetic editing techniques allows the construction of reporter lines (for example, GFP) fused to specific genes [6]. One of the main tools that make the fruit fly an excellent model organism is the possibility of expressing genes of interest in specific tissues through the UAS-GAL4 binary expression system. This system consists of two factors: the GAL4 transcription factor fused to the promoter region of a gene of interest and the upstream activation sequence (UAS). GAL4 is able to bind the upstream activation sequence (UAS), activating the transcription of a target gene linked to UAS, allowing ectopic gene expression [6]. Thus, the use of fluorescent reporter genes under the control of the UAS-GAL4 system allows a degree of specificity necessary to monitor cellular and biochemical phenomena *in vivo* in different tissues, such as autophagy, [7] mitophagy [8], and changes in the redox state of cells [1]. Taken together, these features are essential for studies that evaluate the effects of xenobiotics on development, however, it can still be improved in the nanotoxicology area, mainly in the use of reporter lines for the elucidation of cellular mechanisms responsible for toxicity and the subcellular localization of nanocrystals.

The development of different nanoscale materials has increased for different applications. Titanium dioxide (TiO_2) nanocrystals (NCs) have been used in several types of cosmetics, food, and the textile industry [9, 10]. This is because this NC has a wide variety of properties that improve materials, such as its bioluminescence and chemical stability [11]. Bioluminescent techniques are widely used in biomedicine for studies of drug screening, molecular markers, and monitoring of molecular reactions, among other applications [12]. Bioluminescent NCs, such as TiO2, present an excellent opportunity to obtain ultra-sensitive and enhanced analyzes and images, in addition to allowing the study of bioluminescence [13–15]. The use of bioluminescent imaging in vivo allows the visualization of biological processes in intact living organisms, providing abundant quantitative space–time information beyond the reach of conventional in vitro tests and fixed material [15].

Doping is a technique that allows the incorporation of substitutional ions into the crystalline structure of materials, generating exciting properties [16]. TiO_2 nanocrystals (NCs) with europium ions incorporated in their structure can be visualized in red fluorescence [17]. This acquired property makes it possible to track luminescence, thus being able to be coupled to biomolecules and drugs for studies of effects and tracking them, for example, which can assist in the studies of

quantitative monitoring of molecular reactions and cellular behaviors, allowing a better understanding of the functions dynamic and complicated biological phenomena [18, 19].

Quantum dots (QDs) of cadmium chalcogenides (CdSe, CdS, and CdTe) absorb and emit in the visible electromagnetic spectrum, and for this reason, they are used in several applications of biological and biomedical marking, such as fluorescent probes, biosensors, and others. In the area of biological labeling, the great applicability of QDs occurs because they present several advantages over traditional organic fluorophores, such as a long fluorescence life span, ~ 100 times greater, which allows to distinguish it from the background b signal, seen that autofluorescence has a much shorter fluorescence life; absorption and emission spectra tunable; high photo resistance and chemo-degradation; and high fluorescence intensity [20–22]. However, this comparison of the fluorescence intensity of the QDs was performed in non-aqueous solvents, with unconjugated QDs, and in non-biological media, since the fluorescence intensity may be lower when the QDs are conjugated and used in biological labeling experiments [23].

Ultra-small PQs (USPQs) are nanocrystals with extremely small sizes, presenting strong quantum confinement effects, in which most of their atoms are located on the surface [24]. A large number of atoms on the surface and the presence of several pendant bonds lead to changes in the properties of nanocrystals, which can be observed in the fluorescence spectra [25].

The quantum dots of magic-sized (MSQDs) are nanocrystals with extremely small sizes (<2 nm) and that present physical property utterly different from traditional QDs [26]. Although MSQDs have similar properties to USQDs, including composition and size, some fundamental properties place these QDs in different classes. The characteristic properties of MSQDs are thermodynamically stable structures, wide luminescence range, high size stability over time, relatively narrow absorption spectra and/or heterogeneous (discontinuous) growth [27–31]. The structures are thermodynamically stable; they are formed from the arrangement of a certain number of atoms, which gives it high stability. Nguyen et al. made theoretical predictions of different types of CdSe MSQDs structures aligned with the literature's experimental results [32]. The term magic size is related to a (magic) number of atoms in the structure that makes QDs extremely stable [32]. The broad luminescence spectrum occurs due to MSQDs having internal atomic defects (absence or extra presence of atoms) [27, 29, 32].

The development of new alternatives for the study of biomolecules in organic systems has grown considerably. The high specificity and sensitivity of scientific methodologies based on fluorescence clarify biological events [33]. Fluorescent probes based on organic dyes have been shown to identify biomolecules [34, 35]. Silva et al. demonstrated that the biocompatibility of CdSe/CdS MSQRd could be tuned in the synthesis, [36] present high luminescence stability in biological systems [37], can be bioconjugated with several biomolecules aiming at the most diverse luminescent probes [38–42] and in biosensors [43, 44].

This chapter shows recent results that the group has been working with fluorescent reporter proteins and the applicability of nanocrystals as fluorescent markers. Nanocrystals of pure and europium doped TiO_2 and CdSe/CdS (MSQDs) will be some of the exciting tools for marking in biological systems.

2. Fluorescent proteins and nanocrystals

This section will show the group results using GFP tagged proteins and nanocrystals' applicability as fluorescent markers.

2.1 Drosophila lines expressing fluorescent proteins

In 2011, Albrecht et al. established a monitoring system that allows assessing the status of chemically defined redox species (the redox pair GSH/GSSH and H_2O_2) in subcellular compartments cytosol and mitochondria *in vivo*. They have fused a probe sensitive to redox changes (ro-GFP2) [45–47] to the microbial H_2O_2 sensor oxidant receptor peroxidase 1 (Orp1) [46]. In a reduced state, this probe exhibits excitation around 488 nm, while upon oxidation, roGFP2 gains excitability at 405 nm and loses excitability at 488 nm. In the present work, we used one of the transgenic *Drosophila* lines described by Albrecht and collaborators, called mito-roGFP2-Orp1 [1] to exemplify how *in vivo* sensors can be valuable for analyzing the redox state and to propose its use for the analysis of nanomaterials biocompatibility *in vivo*. In **Figure 1** we show different dissected larval tissues of *Drosophila*

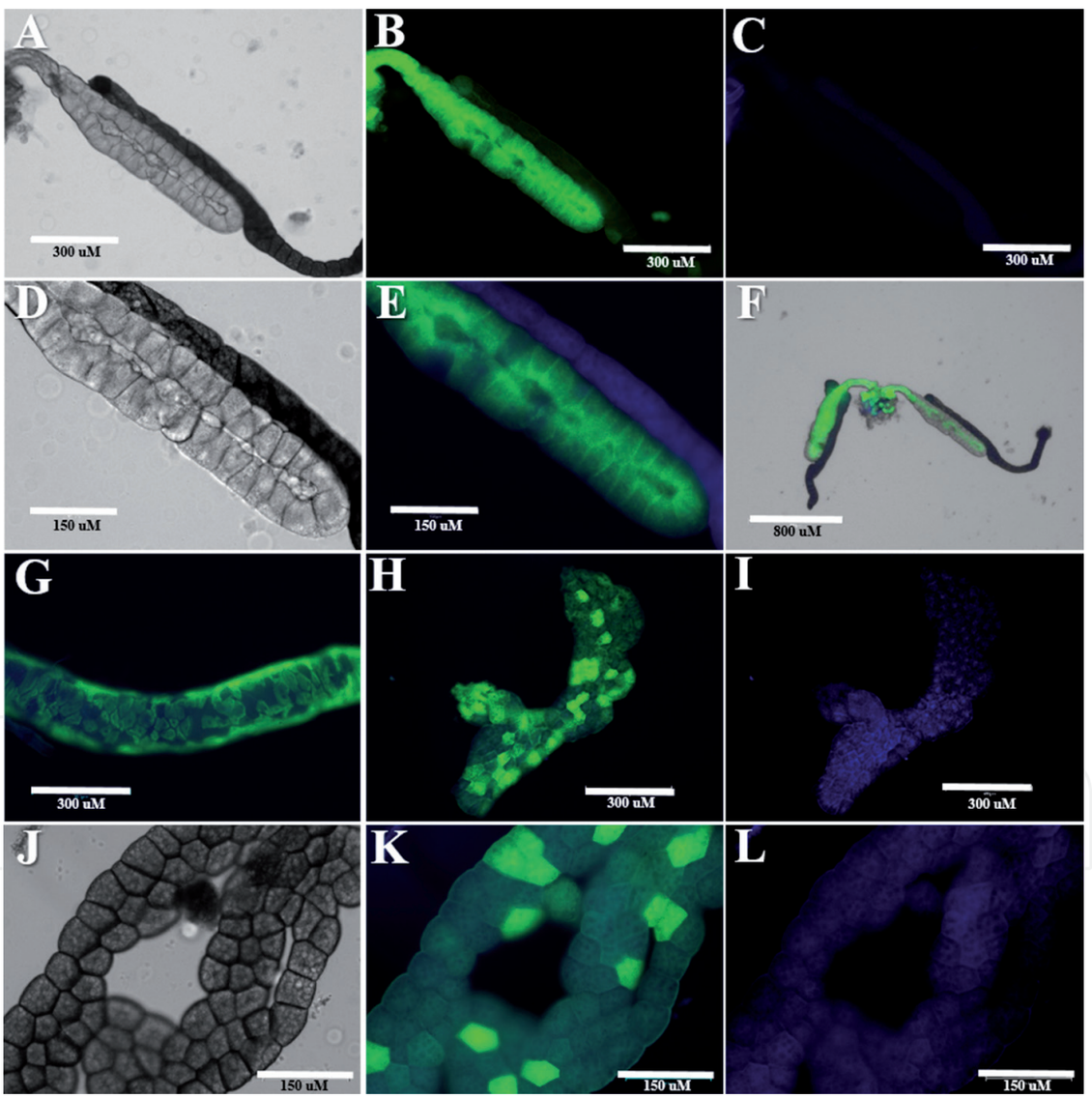

Figure 1.
Drosophila *lines expressing fluorescent proteins can be used as* in vivo *sensors of redox status. Different GAL4 drivers were used to express Mito-orp1-GFP in different* Drosophila *larval tissues. (A-F) The* Drosophila *GAL4 driver sgs3-GAL4 was used to express Mito-orp1-GFP2 in larval salivary glands. A- bright field image of a* Drosophila *larval salivary gland. In (B) the Mito-orp1-GFP can be visualized in its reduced state, while in (C) a weak signal is seen under 405 nm light. A greater magnification of the salivary gland shown in a can be seen in (D) while in (E) the overlap of the Mito-orp1-GFP2 in its reduced (488 nm) and oxidized (405 nm) state is shown. (G) Larval midgut showing the overlap of the Mito-orp1-GFP2 in its reduced (488 nm) and oxidized (405 nm) state. The Mito-orp1-GFP2 in its reduced state is shown in (H) and (K) while the sensor oxidized fluorescence is seen in (I) and (L). All images were acquired using ThermoFisher Scientific EVOS M7000 Imaging System.*

expressing the redox sensor mito-roGFP2-Orp1. **Figure 1A** shows the bright field image of a dissected larval salivary gland, while in 3B we can see that there is a high concentration of mito-roGFP2-Orp1 in its reduced state, evidenced by green fluorescence, and a low concentration of mito-roGFP2-Orp1 in its oxidized state. In 1D, a higher magnification image of the salivary gland in 1A is shown, while in 1E the merged image of 488 nm and 405 nm channels shows the balance between reduced and oxidized mito-roGFP2-Orp1. In 1G, a portion of the midgut also shows a higher concentration of reduced mito-roGFP2-Orp1. **Figure 1H** shows reduced mito-roGFP2-Orp1 distribution throughout the larval fat body. It is interesting to notice that there is a clear difference in the concentration of reduced mito-roGFP2-Orp1 in cells within the same tissue, which is even more evident in the image in greater magnification shown in 1 K. The samples in 1I and 1 L show the oxidized mito-roGFP2-Orp1 in the same larval fat body. As expected, our analysis of control samples showed that most mito-roGFP2-Orp1 proteins are in its reduced state, exhibiting excitation around 488 nm. We are currently using this valuable tool to analyze the effect of different nanocrystals on the redox balance in *Drosophila* as an additional approach for the determination of biocompatibility *in vivo*.

Figure 2 shows three different transgenic lines of *Drosophila* that can be used to assist in the subcellular localization of fluorescent nanoparticles. **Figure 2A-C** shows dissected tissues of the D1-GFP transgenic line (BL.66454). The D1-GFP protein binds to chromosomes allowing the nuclei visualization. In **Figure 2A** we can see a pair of larval salivary glands while **Figure 2B-C** shows different portions of the larval gut. The progeny of the cross between the lineage mef2-Gal4 and UAS-mito-GFP (BL. 8443) was used to visualize the larval muscles (**Figure 2D-F**). This is because mef2-Gal4 drives Gal4 expression in muscles where it binds to the regulatory sequence UAS-mito-GFP, which in turn regulates the expression of a

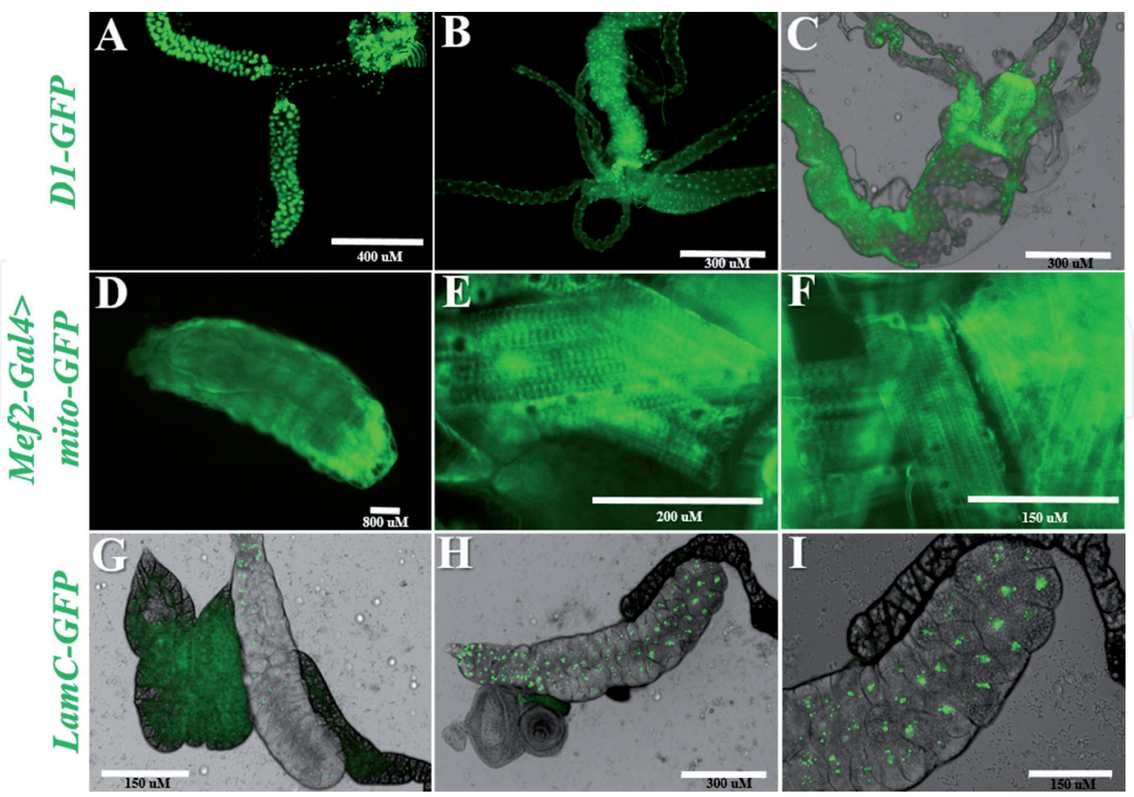

Figure 2.
The expression of fluorescent proteins in Drosophila *as a tool to visualize cellular subcompartments. (A-C) D1-GFP expression in* Drosophila *larval tissues. A pair of larval salivary glands is shown in a while (B) and (C) shows different portions of the larval gut. (D-F) L3 larvae expressing Mito-GFP in muscles. (G-I) shows salivary glands expressing LamC-GFP localization at the nuclear envelope of cells.*

mitochondrial import sequence fused to the fluorescent protein GFP, allowing the visualization of mitochondria in the muscle tissues. **Figure 2G-I** shows salivary glands of the LamC-GFP transgenic lineage (BL. 6837) which allows for the visualization of the nuclear envelope of cells. In these examples, we showed 3 different *Drosophila* transgenic lines in the green band (GFP) that can be used to assist in the subcellular localization of fluorescent nanoparticles, however, it is essential to notice that hundreds of lines are available. Data on the genome and the wide range of reporter lines of *Drosophila* can be found on Flybase (https://flybase.org/). Reporter lines of *Drosophila* can be purchased in collections such as Bloomington *Drosophila* Stock Center (BDSC) at Indiana University. These different tools allow the investigators to choose from a great variety of cell types, subcellular compartments as well as the fluorescence band that best adapts to the nanoparticles of interest.

2.2 Nanocrystals as luminescent markers (nanomarkers)

Figure 3 shows exciting results on pure and europium (Eu) doped TiO_2 NCs. TiO_2 NCs absorb and emit in the ultraviolet, but when incorporating the europium ions in its crystalline structure, by replacing some titanium ions, it shows luminescence in red. The colors emitted by the pure and Eu doped TiO_2 NCs (**Figure 3a**), and the crystalline structure in the anatase phase (**Figure 3b**) are illustrated. Also, in **Figure 3c**, the emission spectra of these nanocrystals are observed.

In order to investigate whether TiO_2 and TiO_2:Eu nanocrystals could be tracked on adult *Drosophila* after exposure during development TiO_2 and TiO_2:Eu nanocrystals were mixed in standard *Drosophila* culture medium at the final concentration of 100 mM.. The larvae were carefully staged and transferred as L1 (first instar larvae) to medium containing TiO_2 and TiO_2:Eu. The control contained only a standard *Drosophila* culture medium. The animals developed through all larval stages during the following 3 days. At this stage, the larvae actively feed until they become pupae. After pupal metamorphosis, the animals emerged as adults were dissected and its abdominal fat body was analyzed through fluorescence microscopy under UV light to analyze the TiO_2 bioaccumulation and under red light to detect TiO_2:Eu. All samples images were acquired using the same light intensity and exposure time. **Figure 4** shows the tracking data of TiO_2 and TiO_2:Eu in the fat body of adult animals after exposure during the larval stage. It is possible to observe that the fat body spheres of the control animals (**Figure 4A** and **C**) show intrinsic fluorescence when excited with ultraviolet light, however when the animals were exposed to TiO_2 the intensity of fluorescence was significantly higher (**Figure 4B** and **D**).

In order to distinguish between intrinsic fluorescence from fat body and TiO_2 fluorescence, the pixel intensity was measured and compared among all fat body spheres of control images and TiO_2 treated samples. As we can observe in the graphic in **Figure 5a** there was a drastic increase in fluorescence due to the presence of TiO_2. The fat body spheres of the control animals (**Figure 4E** and **G**) also showed intrinsic fluorescence when excited with red light; however, when the animals have exposed to TiO_2:Eu the intensity of fluorescence was higher (**Figure 4F** and **H**). The pixel intensity analysis showed that the presence of TiO_2:Eu caused a significant increase in fluorescence (**Figure 5b**). The observation that the NCs of TiO_2 and TiO_2:Eu could be detected in the fat body of newly emerged adult animals indicates that the bioaccumulation of nanocrystals during larval development persisted until the beginning of the adult stage. Surprisingly, we observed that animals dissected on the second day of its emergence no longer had fat bodies fluorescent spheres containing nanocrystals. This may indicate that one day following the emergence, the animals were able to excrete the NC. The disappearance of nanocrystals may

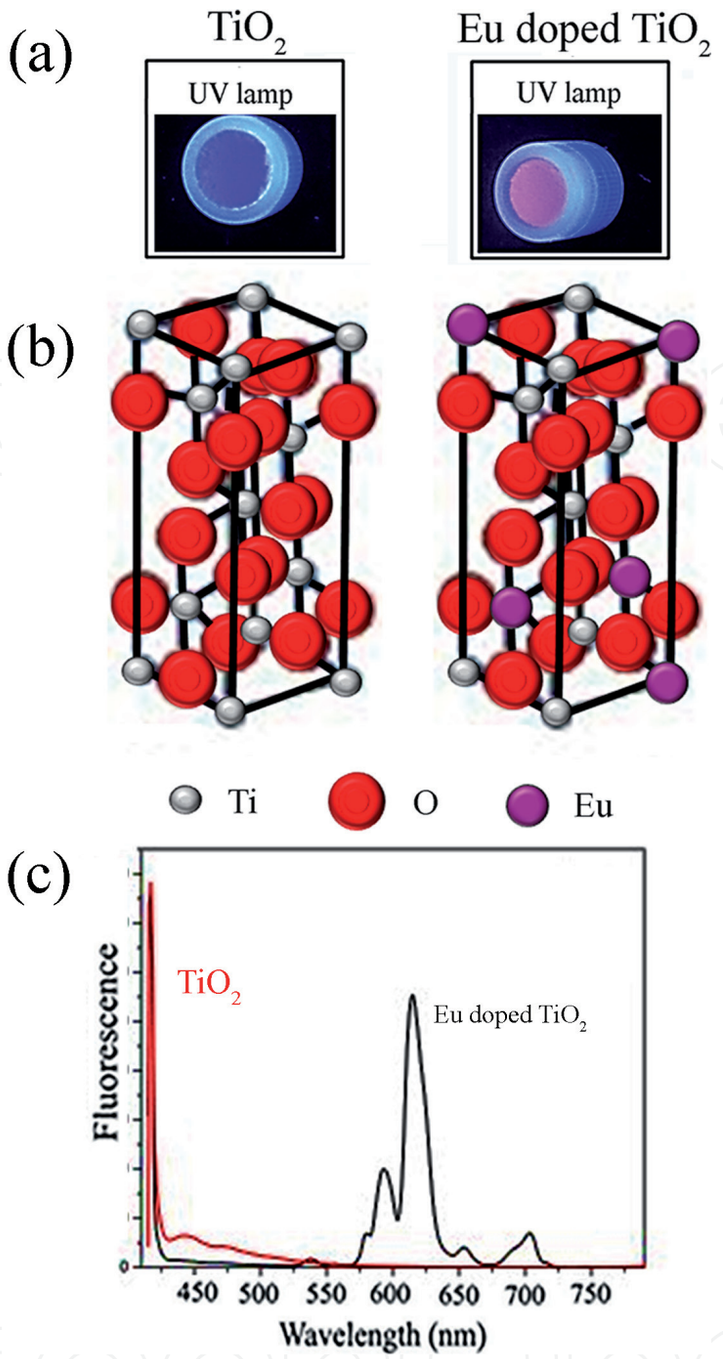

Figure 3.
(a) Photographic image of nanopowders, (b) anatase crystalline structure, (c) luminescence spectra of pure and Eu doped TiO_2 NCs.

also be related to the rapid absorption of the fat body during the first days of life. Similar results were described by Jovanovic et al. 2016, which observed that animals that received TiO_2 during the larval stage did not have TiO_2 as adults [9].

The optical properties and illustration of CdSe/CdS are shown in **Figure 6**. The aqueous solution and the illustration of the core/shell structure of CdSe/CdS MSQDs with a surfactant are exemplified to facilitate understanding (**Figure 6a, b**). The optical absorption and broad luminescence spectra are characteristics of magic-sized quantum dots of CdSe/CdS (**Figure 6c**). In addition, one of the essential properties of the CdSe/CdS MSQDs that allows its application in biological systems is entering and staying inside cells. To test this capacity, we incubated a classical macrophage cell line (RAW 264.7) with CdSe/CdS MSQDs of (200 ng/μL) and evaluated their internalization by Flow Cytometry in different time points (1 to 60 minutes). Flow

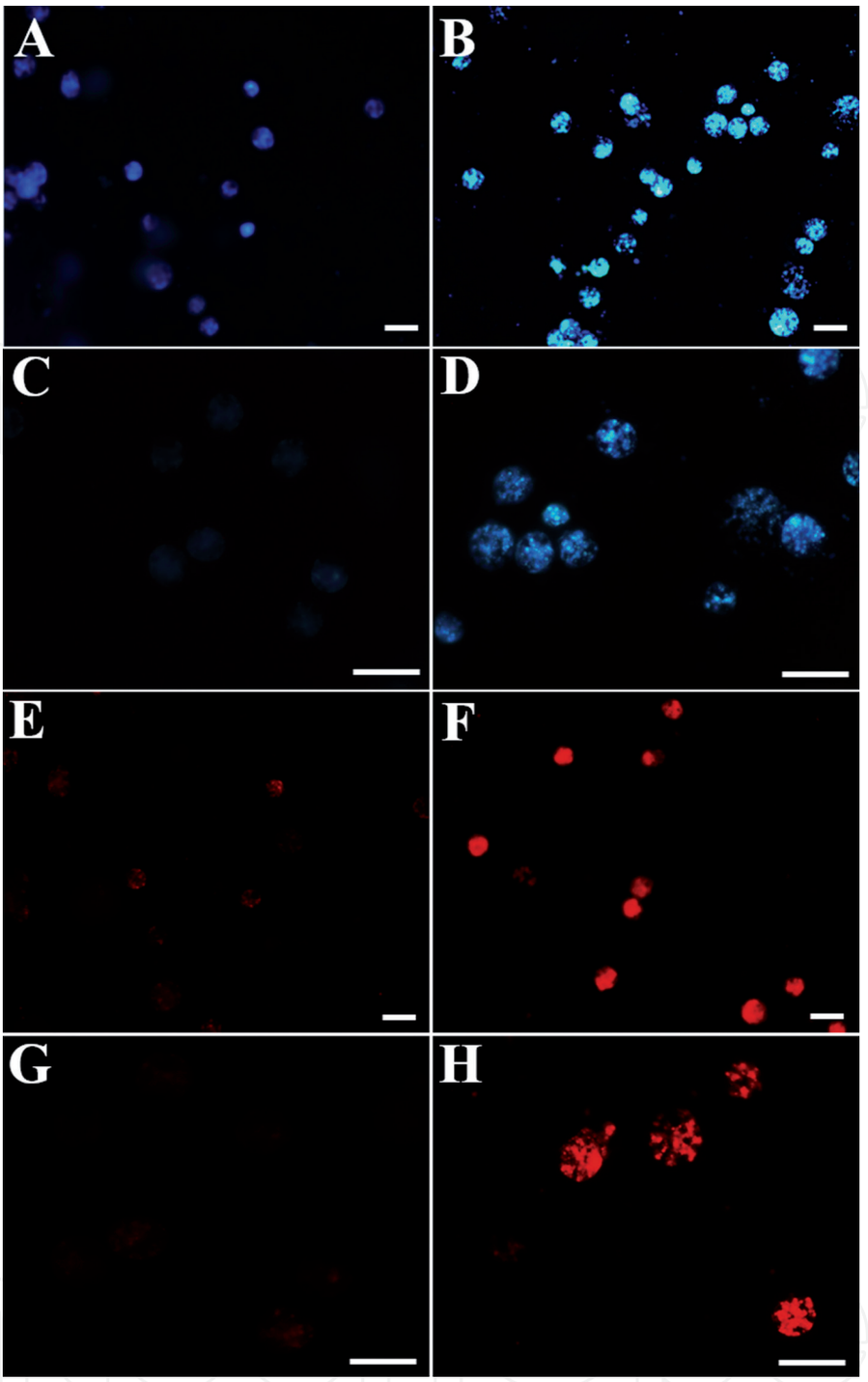

Figure 4.
In vivo *fluorescence of TiO_2 and TiO_2:Eu in adult* Drosophila *fat body.* Drosophila *tissues as the fat body shows a well-known intrinsic fluorescence as observed in representative images of control animals (A) and (C) at 405 nm E and G at 546 nm), however in the TiO_2 (B and D) and TiO_2:Eu (F and H) treated animals it is possible to observe a drastic increase in luminescence when compared to control. Scale bar represents 50uM.*

Cytometry is a unique methodological approach to determine cell staining as it evaluates a considerable number of cells per second, one by one, and reports if cells are fluorescent. Just after 1 minute, the MSQDs nearly 50% of cells were fluorescent, and this percentual was growing to >97% after 60 minutes (**Figure 6c, d**).

Bioimaging assays are biological applications QDs since they can be bioconjugated with proteins, antibodies, and DNA [39, 48, 49]. In general, these tests depend on the biocompatibility of QDs, which is obtained by functionalizing the surface of these nanoparticles [39, 50–52]. The bioconjugation allows the study and tracking of biomolecules in biological systems such as cell cultures

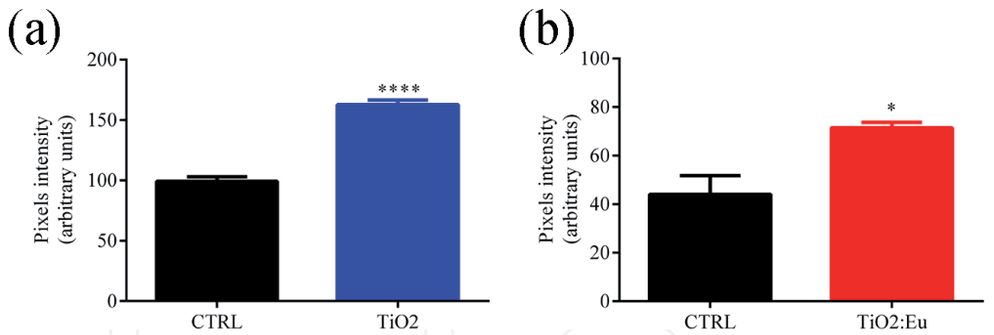

Figure 5.
Indirect quantification of TiO_2 and TiO_2:Eu fluorescence. (a) Pixel intensity analysis of fat body spheres of TiO_2 treated Drosophila *to control fat body spheres. (b) Pixel intensity analysis of fat body spheres of TiO_2:Eu treated animals compared to control fat body spheres.*

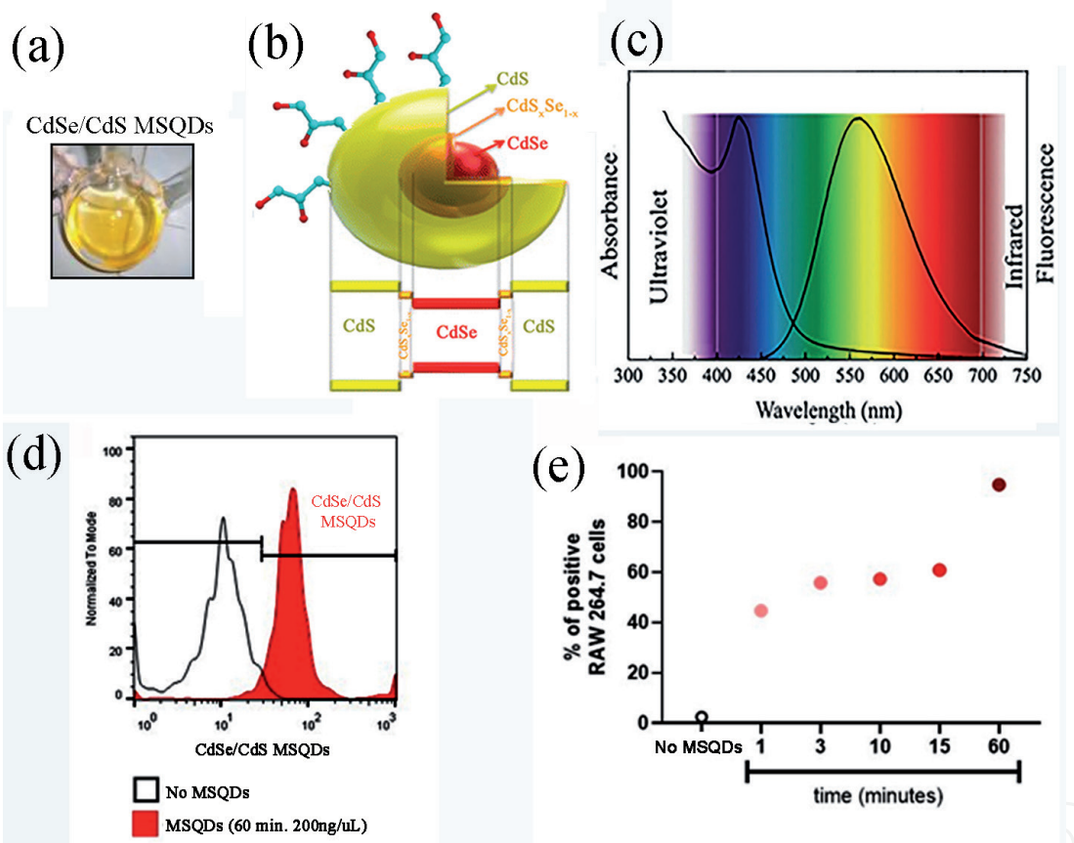

Figure 6.
(a) Photographic image of solution, (b) illustration of CdSe/CdS MSQDs, (c) optical absorption/luminescence spectra of CdSe/CdS MSQDs (d, e) incorporation of MSQDs by RAW 264.7. The intracellular location was determined by flow cytometry after incubation of CdSe/CdS MSQDs (200 ng/uL) with RAW 264.7 cell line (1x10^4/mL) at different time points. Cells were washed in saline solution before acquisition to exclude extracellular MSQDs. At least 5000 events were acquired in a FacsCalibur flow cytometer.

and laboratory animals [53, 54]. The versatility of QDs associated with maltose-binding protein for intracellular delivery of the drug beta-cyclodextrin [55]. Other studies have used the quantum dots for *in vivo* multiphoton biologic imaging. Kwon et al. conjugated iron selenide QDs with monoclonal human epidermal growth factor receptor 2 antibodies to study xenograft breast tumor model in mice [56].

The tracking and study of biomolecules labeled with QDs in vitro and in vivo is a reality in several areas, allowing us to analyze the location and distribution of bioconjugate in biological systems. Silva et al. demonstrated that the CdSe/CdS MSQDs could be bioconjugated with several biomolecules aiming at the most

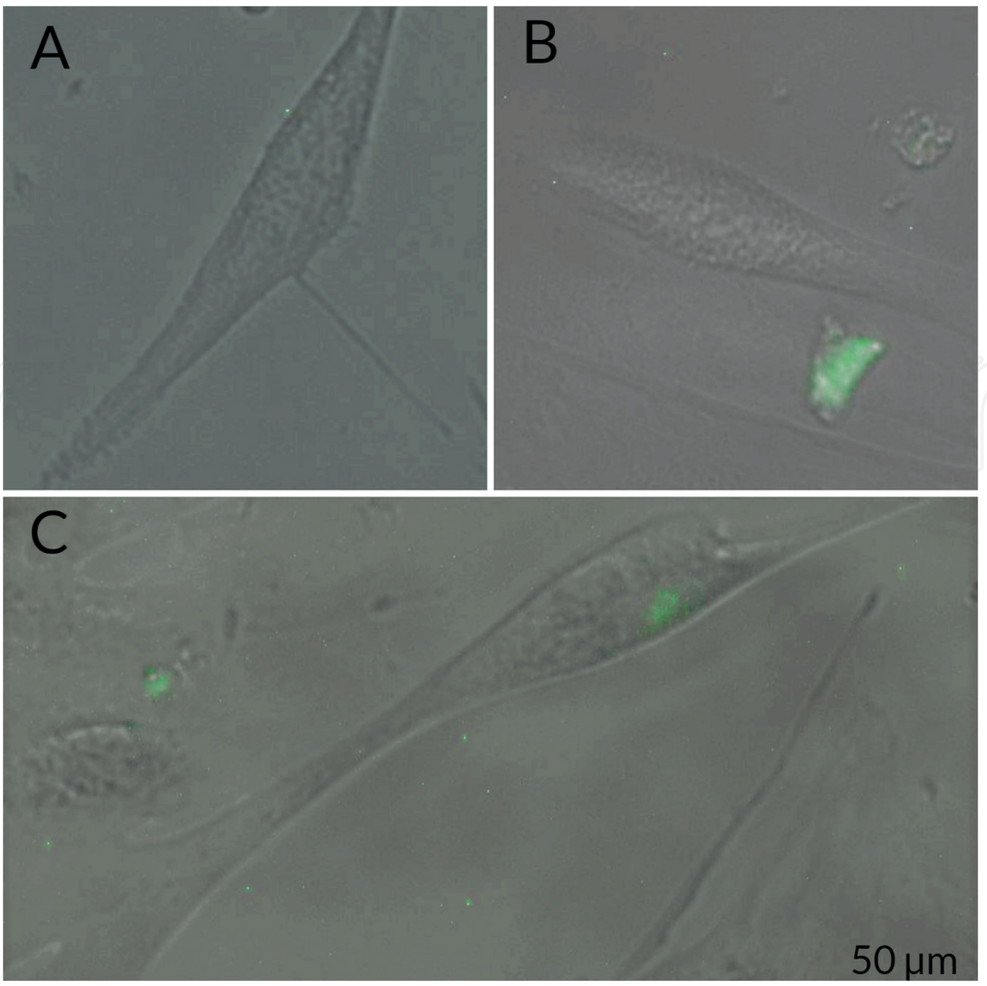

Figure 7.
Fluorescence microscopy images showing the tracking of BaltPLA$_2$ in myoblast culture. (A) Cell control (myoblasts only); (B) myoblasts treated with MSQDs (200 ng/μL) for 18 h; (C) myoblasts treated with MSQDs (200 ng/μL)-BaltPLA$_2$ (100 ng/μL) for 18 h. scale 50 μm.

diverse luminescent probes [38–42] in biosensors [43, 44]. Dias et al. labeled a phospholipase A2 isolated from *Bothrops alternatus* snake venom with CdSe/CdS MSQDs to track it in myoblast culture, making it possible to identify the bioconjugate on the surface of the plasma membrane and in the nuclear region [39]. **Figure 7** corroborates these data since it is possible to observe fluorescence markings only in myoblasts treated with the bioconjugate MSQDs-BaltPla2.

3. Conclusion

In this chapter, we have shown that fluorescent reporter proteins in the *Drosophila* model system are excellent tools to monitor cellular and biochemical phenomena *in vivo*, such as changes in the redox state of cells, as well as are a valuable tools to assist in the subcellular localization of fluorescent nanoparticles. We also showed that TiO_2 and Eu doped TiO_2 NCs fluorescence could be detected in adult animals following exposure during development. Intracellular location of CdSe/CdS MSQDs in RAW 264.7 cell line and tracking of BaltPLA$_2$ bioconjugated in myoblast culture. Therefore, the use of fluorescent proteins and nanocrystals *in vivo* are exciting tools as they provide abundant qualitative and quantitative data and allow the visualization of biological processes in intact cells and living organisms.

Acknowledgements

This work was supported by grants of CNPq, CAPES, FAPEAL, and FAPEMIG.

Conflict of interest

The authors declare no conflict of interest.

Author details

Anielle Christine Almeida Silva[1,2*], Jerusa Maria de Oliveira[3], Kelen Talita Romão da Silva[1,3], Francisco Rubens Alves dos Santos[1,3], João Paulo Santos de Carvalho[1], Rose Kethelyn Souza Avelino[3], Eurípedes Alves da Silva Filho[4], Marcelo Duzzioni[5], Edigar Henrique Vaz Dias[6], Fábio de Oliveira[7], Juliana Rodrigues Machado[8], Malu Mateus Santos[9], Marcos Vinícius da Silva[9], Carlo José Freire de Oliveira[9], Virmondes Rodrigues Junior[9], Lucas Anhezini[3] and Noelio Oliveira Dantas[1*]

1 Laboratory of New Nanostructured and Functional Materials, Physics Institute, Federal University of Alagoas, Maceió, Alagoas Brazil

2 Programa de Pós-Graduação da Rede Nordeste de Biotecnologia (RENORBIO), Federal University of Alagoas, Maceió, Alagoas Brazil

3 Laboratory for in vivo Toxicity, Institute of Biological Sciences and Health, Federal University of Alagoas, Maceió, Alagoas, Brazil

4 Laboratory of Genetic and Applied Microbiology, Institute of Biological Sciences and Health, Federal University of Alagoas, Maceió, Alagoas, Brazil

5 Laboratory of Pharmacological Innovation, Institute of Biological Sciences and Health, Federal University of Alagoas, Maceió, Alagoas, Brazil

6 State University of Minas Gerais, Ituiutaba, MG, Brazil

7 Institute of Biomedical Sciences, Federal University of Uberlândia, Uberlândia, MG, Brazil

8 Department of Pathology, Genetics and Evolution, Federal University of Triângulo Mineiro, Uberaba, Minas Gerais, Brazil

9 Department of Microbiology, Immunology, and Parasitology, Institute of Biological and Natural Sciences, Federal University of Triângulo Mineiro, Uberaba, MG, Brazil

*Address all correspondence to: aniellechristineas@gmail.com and noelio@fisufal.br

IntechOpen

References

[1] Albrecht, S.C.; Barata, A.G.; Großhans, J.; Teleman, A.A.; Dick, T.P. In vivo mapping of hydrogen peroxide and oxidized glutathione reveals chemical and regional specificity of redox homeostasis. *Cell Metab.* 2011, *14*, 819-829, doi:10.1016/j.cmet.2011.10.010.

[2] Chudakov, D.M.; Matz, M. V.; Lukyanov, S.; Lukyanov, K.A. Fluorescent proteins and their applications in imaging living cells and tissues. *Physiol. Rev.* 2010, *90*, 1103-1163, doi:10.1152/physrev.00038.2009.

[3] VanEngelenburg, S.B.; Palmer, A.E. Fluorescent biosensors of protein function. *Curr. Opin. Chem. Biol.* 2008, *12*, 60-65, doi:10.1016/j.cbpa.2008.01.020.

[4] Ong, C.; Yung, L.Y.L.; Cai, Y.; Bay, B.H.; Baeg, G.H. Drosophila melanogaster as a model organism to study nanotoxicity. *Nanotoxicology* 2015, *9*, 396-403, doi:10.3109/17435390.2014.940405.

[5] Pandey, U.B.; Nichols, C.D. Human disease models in *Drosophila melanogaster* and the role of the fly in therapeutic drug discovery. *Pharmacol. Rev.* 2011, *63*, 411-436, doi:10.1124/pr.110.003293.

[6] Hales, K.G.; Korey, C.A.; Larracuente, A.M.; Roberts, D.M. Genetics on the fly: A primer on the drosophila model system. *Genetics* 2015, *201*, 815-842, doi:10.1534/genetics.115.183392.

[7] Devorkin, L.; Gorski, S.M. Monitoring autophagy in drosophila using fluorescent reporters in the UAS-GAL4 system. *Cold Spring Harb. Protoc.* 2014, *2014*, 967-972, doi:10.1101/pdb.prot080341.

[8] Kim, Y.Y.; Um, J.H.; Yoon, J.H.; Kim, H.; Lee, D.Y.; Lee, Y.J.; Jee, H.J.; Kim, Y.M.; Jang, J.S.; Jang, Y.G.; et al. Assessment of mitophagy in mt-Keima Drosophila revealed an essential role of the PINK1-Parkin pathway in mitophagy induction in vivo. *FASEB J.* 2019, *33*, 9742-9751, doi:10.1096/fj.201900073R.

[9] Jovanović, B.; Jovanović, N.; Cvetković, V.J.; Matić, S.; Stanić, S.; Whitley, E.M.; Mitrović, T.L. The effects of a human food additive, titanium dioxide nanoparticles E171, on *Drosophila melanogaster* - a 20 generation dietary exposure experiment. *Sci. Rep.* 2018, *8*, 1-12, doi:10.1038/s41598-018-36174-w.

[10] Chen, X.; Mao, S.S. Titanium dioxide nanomaterials: Synthesis, properties, modifications and applications. *Chem. Rev.* 2007, *107*, 2891-2959.

[11] Kamat, P. V. *Journal of Physical Chemistry C*. 2012, pp. 11849-11851.

[12] Fleiss, A.; Sarkisyan, K.S. A brief review of bioluminescent systems (2019). *Curr. Genet.* 2019, *65*, 877-882, doi:10.1007/s00294-019-00951-5.

[13] Duarte, C.A.; Goulart, L.R.; Filice, letícia de S.C.; De Lima, I.L.; Campos-Fernándes, E.; Dantas, N.O.; Silva, A.C.A.; Soares, M.B.P.; Santos, R.R.; CArdoso, C.M.A.; et al. Characterization of Crystalline Phase of TiO 2. *Materials (Basel).* 2020, *13*, 4071.

[14] Barkalina, N.; Charalambous, C.; Jones, C.; Coward, K. Nanotechnology in reproductive medicine: Emerging applications of nanomaterials. *Nanomedicine Nanotechnology, Biol. Med.* 2014, *10*, e921–e938, doi:10.1016/j.nano.2014.01.001.

[15] Padmanabhan, P.; Kumar, A.; Kumar, S.; Chaudhary, R.K.; Gulyás, B. Nanoparticles in practice for molecular-imaging applications: An overview. *Acta*

Biomater. 2016, *41*, 1-16, doi:10.1016/j.actbio.2016.06.003.

[16] Bharat, T.C.; Shubham; Mondal, S.; Gupta, H.S.; Singh, P.K.; Das, A.K. Synthesis of doped zinc oxide nanoparticles: A review. In Proceedings of the Materials Today: Proceedings; Elsevier Ltd, 2019; Vol. 11, pp. 767-775.

[17] Sandoval, S.; Yang, J.; Alfaro, J.G.; Liberman, A.; Makale, M.; Chiang, C.E.; Schuller, I.K.; Kummel, A.C.; Trogler, W.C. Europium-doped TiO 2 hollow nanoshells: Two-photon imaging of cell binding. *Chem. Mater.* 2012, *24*, 4222-4230, doi:10.1021/cm302642g.

[18] Ghaderi, S.; Ramesh, B.; Seifalian, A.M. Fluorescence nanoparticles "quantum dots" as drug delivery system and their toxicity: A review. *J. Drug Target.* 2011, *19*, 475-486, doi:10.3109/1061186X.2010.526227.

[19] Vollrath, A.; Schubert, S.; Schubert, U.S. Fluorescence imaging of cancer tissue based on metal-free polymeric nanoparticles-a review. *J. Mater. Chem. B* 2013, *1*, 1994-2007, doi:10.1039/c3tb20089b.

[20] Alivisatos, P. The use of nanocrystals in biological detection. *Nat. Biotechnol.* 2004, *22*, 47-52, doi:10.1038/nbt927.

[21] Resch-Genger, U.; Grabolle, M.; Cavaliere-Jaricot, S.; Nitschke, R.; Nann, T. Quantum dots versus organic dyes as fluorescent labels. *Nat Methods.* 2008, *5*, 763-75.

[22] Deerinck, T.J. The application of fluorescent quantum dots to confocal, multiphoton, and electron microscopic imaging. *Toxicol. Pathol.* 2008, *36*, 112-6, doi:10.1177/0192623307310950.

[23] Wu, X.; Liu, H.; Liu, J.; Haley, K.N.; Treadway, J.A.; Larson, J.P.; Ge, N.; Peale, F.; Bruchez, M.P. Immunofluorescent labeling of cancer marker Her2 and other cellular targets with semiconductor quantum dots. *Nat. Biotechnol.* 2002, *21*, 41-46.

[24] Dai, Q.; Li, D.; Chang, J.; Song, Y.; Kan, S.; Chen, H.; Zou, B.; Xu, W.; Xu, S.; Liu, B.; et al. Facile synthesis of magic-sized CdSe and CdTe nanocrystals with tunable existence periods. *Nanotechnology* 2007, *18*, 405603, doi:10.1088/0957-4484/18/40/405603.

[25] Murray, C.B.; Kagan, C.R.; Bawendi, M.G. Synthesis and Characterization of Monodisperse Nanocrystals and Close-Packed Nanocrystal Assemblies. *Annu. Rev.Mater* 2000, *30*, 545.

[26] Chen, X.; Samia, A.C.S.; Lou, Y.; Burda, C. Investigation of the crystallization process in 2 nm CdSe quantum dots. *J. Am. Chem. Soc.* 2005, *127*, 4372-4375, doi:10.1021/ja0458219.

[27] Riehle, F.S.; Bienert, R.; Thomann, R.; Urban, G.A. Blue Luminescence and Superstructures from Magic Size Clusters of CdSe. *Nano Lett.* 2009, *9*, 514-518, doi:10.1021/nl080150o.

[28] McBride, J.R.; Dukes, A.D.; Schreuder, M. a; Rosenthal, S.J. On Ultrasmall Nanocrystals. *Chem. Phys. Lett.* 2010, *498*, 1-9, doi:10.1016/j.cplett.2010.08.052.

[29] Dukes, A.D.; McBride, J.R.; Rosenthal, S.J. Synthesis of Magic-Sized CdSe and CdTe Nanocrystals with Diisooctylphosphinic Acid. *Chem. Mater.* 2010, *22*, 6402-6408, doi:10.1021/cm102370a.

[30] Bowers, M.J.; McBride, J.R.; Rosenthal, S.J. White-light emission from magic-sized cadmium selenide nanocrystals. *J Am Chem Soc* 2005, *127*, 15378-15379.

[31] Harrell, S.M.; McBride, J.R.; Rosenthal, S.J. Synthesis of ultrasmall and magic-sized CdSe nanocrystals. *Chem. Mater.* 2013, *25*, 1199-1210.

[32] Nguyen, K.A.; Day, P.N.; Pachter, R. Understanding structural and optical properties of nanoscale CdSe magic-size quantum dots: Insight from computational prediction. *J. Phys. Chem. C* 2010, *114*, 16197-16209, doi:10.1021/jp103763d.

[33] Shashkova, S.; Leake, M.C. Single-molecule fluorescence microscopy review: Shedding new light on old problems. *Biosci. Rep.* 2017, *37*, BSR20170031, doi:10.1042/BSR20170031.

[34] Martynov, V.I.; Pakhomov, A.A.; Popova, N. V.; Deyev, I.E.; Petrenko, A.G. Synthetic Fluorophores for Visualizing Biomolecules in Living Systems. *Acta Naturae* 2016, *8*, 33-46, doi:10.32607/20758251-2016-8-4-33-46.

[35] Yan, F.; Fan, K.; Bai, Z.; Zhang, R.; Zu, F.; Xu, J.; Li, X. Fluorescein applications as fluorescent probes for the detection of analytes. *TrAC - Trends Anal. Chem.* 2017, *97*, 15-35, doi:10.1016/j.trac.2017.08.013.

[36] Almeida Silva, A.; Silva, M.J.; da Luz, F.A.; Silva, D.; de Deus, S.; Dantas, N. Controlling the Cytotoxicity of CdSe Magic-Sized Quantum Dots as a Function of Surface Defect Density. *Nano Lett. 14*, 5452-5457, doi:10.1021/nl5028028.

[37] Silva, A.C.A.; Deus, S.L.V. De; Silva, M.J.B.; Dantas, N.O. Highly stable luminescence of CdSe magic-sized quantum dots in HeLa cells. *Sensors Actuators, B Chem.* 2014, *191*, 108-114, doi:10.1016/j.snb.2013.09.063.

[38] Silva, A.C.A.; Dantas, N.O.; Silva, M.J.B.; Spanó, A.M.; Goulart, ; Luiz Ricardo Functional Nanocrystals : Towards Biocompatibility , Nontoxicity and. In *Advances in Biochemistry & Applications in Medicine*; 2017; pp. 1-27.

[39] Dias, E.H.V.; Pereira, D.F.C.; de Sousa, B.B.; Matias, M.S.; de Queiroz, M.R.; Santiago, F.M.; Silva, A.C.A.; Dantas, N.O.; Santos-Filho, N.A.; de Oliveira, F. In vitro tracking of phospholipase A 2 from snake venom conjugated with magic-sized quantum dots. *Int. J. Biol. Macromol.* 2019, *122*, 461-468, doi:10.1016/j.ijbiomac.2018.10.185.

[40] Silva, A.C.A.; Correia, L.I.V.; Silva, M.J.B.; Zóia, M.A.P.; Azevedo, F.V.P.V.; Rodrigues, Jéssica Peixoto Goulart, L.R.; Ávila, Veridiana de Melo Dantas, N.O. Biocompatible Magic Sized Quantum Dots: Luminescent Markers and Probes. In; Correia, L.I.V., Ed.; IntechOpen: Rijeka, 2018; p. Ch. 6 ISBN 978-1-78923-295-0.

[41] Silva, A.C.A.; Azevedo, F.V.P.V.; Zóia, M.A.P.; Rodrigues, J.P.; Dantas, N.O.; Melo, V.R.Á.; Goulart, L.R. Magic Sized Quantum Dots as a Theranostic Tool for Breast Cancer. In *Recent Studies & Advances in Breast Cancer*; Open Access eBooks: Wilmington, 2017; pp. 1-10 ISBN 978-81-935757-2-7.

[42] Silva, A.C.A.; Neto, E.S.F.; Da Silva, S.W.; Morais, P.C.; Dantas, N.O. Modified phonon confinement model and its application to CdSe/CdS core-shell magic-sized quantum dots synthesized in aqueous solution by a new route. *J. Phys. Chem. C* 2013, doi:10.1021/jp308500r.

[43] de França, C.C.L.; Meneses, D.; Silva, A.C.A.; Dantas, N.O.; de Abreu, F.C.; Petroni, J.M.; Lucca, B.G. Development of novel paper-based electrochemical device modified with CdSe/CdS magic-sized quantum dots and application for the sensing of dopamine. *Electrochim. Acta* 2021, *367*, 137486, doi:10.1016/j.electacta.2020.137486.

[44] de Lima França, C.C.; da Silva Terto, E.G.; Dias-Vermelho, M. V.; Silva, A.C.A.; Dantas, N.O.; de Abreu, F.C. The electrochemical behavior of core-shell CdSe/CdS magic-sized

quantum dots linked to cyclodextrin for studies of the encapsulation of bioactive compounds. *J. Solid State Electrochem.* 2016, *20*, 2533-2540, doi:10.1007/s10008-016-3221-8.

[45] Dooley, C.T.; Dore, T.M.; Hanson, G.T.; Jackson, W.C.; Remington, S.J.; Tsien, R.Y. Imaging dynamic redox changes in mammalian cells with green fluorescent protein indicators. *J. Biol. Chem.* 2004, *279*, 22284-22293, doi:10.1074/jbc.M312847200.

[46] Gutscher, M.; Pauleau, A.L.; Marty, L.; Brach, T.; Wabnitz, G.H.; Samstag, Y.; Meyer, A.J.; Dick, T.P. Real-time imaging of the intracellular glutathione redox potential. *Nat. Methods* 2008, *5*, 553-559, doi:10.1038/nmeth.1212.

[47] Hanson, G.T.; Aggeler, R.; Oglesbee, D.; Cannon, M.; Capaldi, R.A.; Tsien, R.Y.; Remington, S.J. Investigating Mitochondrial Redox Potential with Redox-sensitive Green Fluorescent Protein Indicators. *J. Biol. Chem.* 2004, *279*, 13044-13053, doi:10.1074/jbc.M312846200.

[48] Silva, A.C.A.; Correia, L.I.V.; Silva, M.J.B.; Zóia, M.A.P.; Azevedo, F.V.P.V.; Rodrigues, J.P.; Goulart, L.R.; Ávila, Veridiana de Melo Dantas, N.O. Biocompatible Magic Sized Quantum Dots: Luminescent Markers and Probes. In *State of the Art in Nano-Bioimaging*; 2017; Vol. 1, pp. 95-104 ISBN 9789537619992.

[49] Silva, A.C.A.; Azevedo, F.V.P.V.; Zóia, M.A.P.; Rodrigues, J.P.; Dantas, N.O.; Melo, V.R.Á.; Goulart, L.R. Magic Sized Quantum Dots as a Theranostic Tool for Breast Cancer. In *Recent Studies & Advances in Breast Cancer*; 2017 ISBN 978-81-935757-2-7.

[50] Silva, A.C.A.; Freschi, A.P.P.; Rodrigues, C.M.; Matias, B.F.; Maia, L.P.; Goulart, L.R.; Dantas, N.O. Biological analysis and imaging applications of CdSe/CdSxSe1−x/CdS core–shell magic-sized quantum dot. *Nanomedicine Nanotechnology, Biol. Med.* 2016, *12*, 1421-1430, doi:10.1016/j.nano.2016.01.001.

[51] Vlasceanu, G.; Grumezescu, A.M.; Gheorghe, I.; Chifiriuc, M.C.; Holban, A.M. Quantum dots for bioimaging and therapeutic applications. In *Nanostructures for Novel Therapy: Synthesis, Characterization and Applications*; Elsevier Inc., 2017; pp. 497-515 ISBN 9780323461481.

[52] Li, J.; Wu, D.; Miao, Z.; Zhang, Y. Preparation of Quantum Dot Bioconjugates and their Applications in Bio-Imaging. *Curr. Pharm. Biotechnol.* 2010, *11*, 662-671, doi:10.2174/138920110792246582.

[53] Gondim, B.L.C.; da Silva Catarino, J.; de Sousa, M.A.D.; de Oliveira Silva, M.; Lemes, M.R.; de Carvalho-Costa, T.M.; de Lima Nascimento, T.R.; Machado, J.R.; Rodrigues, V.; Oliveira, C.J.F.; et al. Nanoparticle-Mediated Drug Delivery: Blood-Brain Barrier as the Main Obstacle to Treating Infectious Diseases in CNS. *Curr. Pharm. Des.* 2019, *25*, 3983-3996, doi:10.2174/1381612825666191014171354.

[54] Makride, S.C.; Gasbarro, C.; Bello, J.M. Bioconjugation of quantum dot luminescent probes for Western blot analysis. *Biotechniques* 2005, *39*, 501-506, doi:10.2144/000112004.

[55] Field, L.D.; Walper, S.A.; Susumu, K.; Lasarte-Aragones, G.; Oh, E.; Medintz, I.L.; Delehanty, J.B. A Quantum Dot-Protein Bioconjugate That Provides for Extracellular Control of Intracellular Drug Release. *Bioconjug. Chem.* 2018, *29*, 2455-2467, doi:10.1021/acs.bioconjchem.8b00357.

[56] Kwon, J.; Jun, S.W.; Choi, S.I.; Mao, X.; Kim, J.; Koh, E.K.; Kim, Y.H.; Kim, S.K.; Hwang, D.Y.; Kim, C.S.; et al. FeSe quantum dots for in vivo multiphoton biomedical imaging. *Sci. Adv.* 2019, *5*, doi:10.1126/sciadv.aay0044.